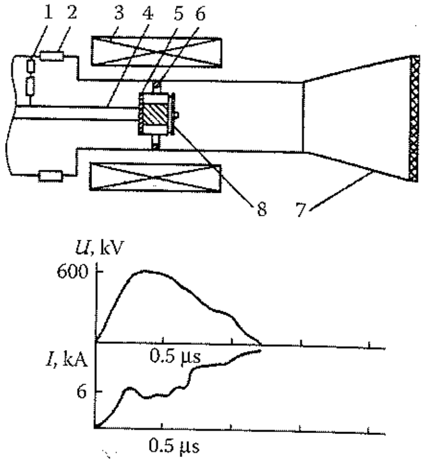

FIGURE 7.31
Long pulse from an inverted magnetron. The elements of the device are the (1) voltage divider, (2) current shunt, (3) solenoid, (4) anode shank, (5) anode, (6) cathode, (7) antenna, and (8) output coupler. (From Vintizenko, I.I. et al., *Sov. Tech. Phys. Lett.*, 13, 256, 1987. With permission.)

and can result in melting and spallation of the surface. Spallation is nonuniform because the rotation of the spokes causes the damage to occur preferentially at one side of the entrance of each resonator, determined by the direction of B_z. Damage is localized on the mid-plane of the resonator. The radial dimensions of a magnetron scale inversely as the frequency f, and the corresponding area over which the energy is deposited scales inversely with f^2, so there is a frequency element to magnetron lifetime as well. Returning to a point made earlier, anode erosion on a large L-band magnetron was not noticeable after thousands of shots, while a C-band magnetron (4.6 GHz) evidenced anode erosion after about 5000 shots, and erosion was severe in X-band magnetrons. To date, specialized materials, such as Elkonite™, tungsten, and other materials that have produced substantial lifetime improvements in high power electrodes in the electrical industry, have not been developed for HPM.

7.6 Fundamental Limitations

In this section, we consider the fundamental limitations of three magnetron parameters: power, efficiency, and frequency.

7.6.1 Power Limits

The output power from a single magnetron is limited fundamentally by a time-dependent analog of the Hull condition, which is defined in the static case in Equation 7.5. Both the RF magnetic field and the external magnetic field are oriented axially, so that insulation fails during a portion of the RF cycle when the peak RF magnetic field cancels the external magnetic field, reducing the total magnetic field to less than B*, the insulating field. In this event, electron loss is enhanced, and the lost electrons strike the anode without producing RF power.

Lemke et al.[18] addressed this issue using computer simulations of rising-sun magnetrons. For a rising-sun magnetron, or for any magnetron with an even number of resonators N, there is a problem with *0-harmonic contamination*, which we explain by noting that the periodicity of the anode structure implies that the electromagnetic fields in the cavity be expanded in a series of the form*

$$B_{zn} = \sum_{m=-\infty}^{\infty} A_m F_m(r) e^{iM(m,n)\theta} e^{-i\omega t} \tag{7.23}$$

where A_m is the amplitude of the mth space harmonic, $F_m(r)$ is a function describing the radial dependence for the space harmonics, and for a rising-sun magnetron operating in the nth mode,

$$M(m,n) = n + m\left(\frac{N}{2}\right) \tag{7.24}$$

The expansion in Equation 7.23 is in a series of spatial harmonics, and when $m = -2n/N$, with N even so that m is an integer (and N is always even for a rising-sun configuration), that particular spatial harmonic has no variation in θ, just like the applied magnetic field insulating the gap. Thus, on one half cycle it reinforces the insulation, and on the other it cancels it. In the reference, the authors consider an N = 14 magnetron and show how the strength of the 0-harmonic contribution depends on the ratio of the depths of the alternating resonators. Further, they show how efficiency declines as the strength of the 0-harmonic contribution grows. Figure 7.32 shows the V-B_z parameter space for the magnetron in the simulations; the operating point for peak power is marked by a solid dot, and the bar through it illustrates the amplitude of the 0-harmonic component of the RF magnetic field. Note that this component of the RF field drives the device below the Hull insulation criterion. This fact is reflected in Figure 7.33, which shows the deposited power from electrons striking the anode; note that the spoke power is disproportionately larger on the half cycle where the 0-harmonic

* This is the application of Floquet's theorem to a system with azimuthal symmetry, just as the slow-wave structures of the Cerenkov devices in Chapter 8 are described using Floquet's theorem for systems with axial symmetry.